HIGH TEMPERATURE MASS SPECTROMETRY OF LIQUID NICKEL-ALUMINIUM ALLOYS

PETER L. MART AND WARREN D. REID

MRL-TR-91-15

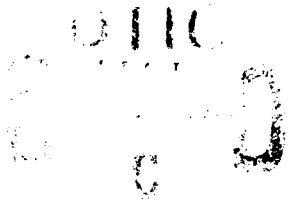

MATERIALS RESEARCH LABORATORY

DSTO

High Temperature Mass Spectrometric Study of the Thermodynamics of Liquid Nickel-Aluminium Alloys at 2000 K

Peter L. Mart and Warren D. Reid

MRL Technical Report
MRL-TR-91-15

Abstract

This report describes a study of the thermodynamic properties of liquid nickel-aluminium alloys, using the technique of Knudsen effusion mass spectrometry. In the concentration range studied, $0.55 \leq x_{Ni} \leq 0.89$, the activity of nickel at 2000 K shows large negative deviations from Raoult's law, which is indicative of the strong attraction between the nickel and aluminium atoms.

The role of container interactions in affecting thermodynamic parameters derived from Knudsen cell measurements is highlighted, and inconsistencies in earlier investigations are discussed.

MATERIALS RESEARCH LABORATORY

Published by

DSTO Materials Research Laboratory
Cordite Avenue, Maribyrnong
Victoria, 3032 Australia

Telephone: (03) 319 3887
Fax: (03) 318 4536

AR No. 006-366

APPROVED FOR PUBLIC RELEASE

Authors

Peter L. Mart

Peter Mart graduated BSc(Hons) (1972) and PhD (1977) in Physical and Inorganic Chemistry from The Flinders University of South Australia. From 1977 to 1979 he was a Research Associate at the Division of Chemistry, National Research Council of Canada, Ottawa. In 1980 he joined MRL and worked in the Materials Division on the thermodynamics and oxidation kinetics of nickel-base superalloys. In 1988 he was attached to the Naval Research Laboratory, Washington DC for 15 months where he worked on sputter-deposited high temperature superconductors. Since returning to MRL he has been involved in research on fuel cell systems.

Warren D. Reid

Warren Reid graduated from The University of Melbourne in 1983 with a BSc(Hons). He joined MRL the same year, working in the High Temperature Properties Group on gas-metals interactions at high temperatures. In 1985 he joined the Ammunition and Armour Metallurgy Group of MRL, working on metallurgical and terminal effectiveness performance of gun launched munitions.

Contents

High Temperature Mass Spectrometric Study of the Thermodynamics of Liquid Nickel-Aluminium Alloys at 2000 K

1. Introduction

Study of the thermodynamic properties of nickel-aluminium alloys is important in providing information on the stability and phase relationships in these alloys, which find numerous applications in high-temperature materials of defence interest.

The phase diagram generally used in the literature is shown in Figure 1, after the critical compilation of Hansen and Anderko [1], and confirmed in subsequent compilations (e.g. [2-4]). However, recent studies by Hilpert *et al.* [5] and Bremer *et al.* [7] have shown a different topology near the Ni_3Al composition, also shown by Figure 1, and confirming earlier work by Schramm [8] rejected by Hansen and Anderko.

Examples of important applications of nickel-aluminium alloys include γ'-Ni_3Al phase precipitation in nickel-base superalloys. This imparts high-temperature strength, necessary for components in the hot end of gas-turbine engines [9]. Diffusion aluminide coatings used to protect nickel-base turbine aerofoils against oxidation and corrosion rely on the formation of the β-NiAl phase. This provides a source of aluminium for growth and repair of the protective scale of alumina which forms at high temperature under oxidizing conditions [10].

The thermodynamic properties of nickel-aluminium alloys are also directly relevant to pyrotechnic compositions containing nickel and aluminium where use is made of the exothermic alloying reaction. Mixtures containing 40 to 80 wt.% Ni can be initiated at ignition temperatures as low as 660°C, are relatively insensitive to shock, impact and vibration, and give exothermic reactions producing temperatures up to at least 2400°C [11]. These are useful for demolition devices, metal cutting and welding, and emergency beacons or flares.

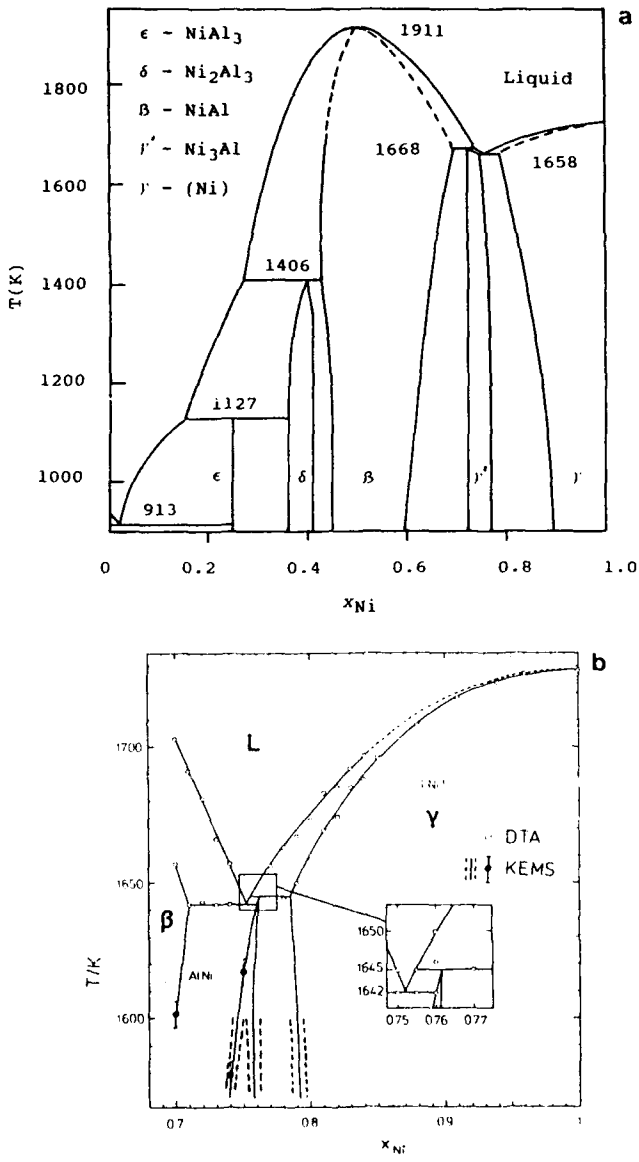

Figure 1: (a) Al-Ni phase diagram according to Hansen and Anderko [1]. (b) Ni rich part of the Al-Ni phase diagram according to Hilpert et al. [5] obtained by Differential Thermal Analysis (DTA) and Knudsen effusion mass spectrometry (KEMS).

The present study was undertaken to resolve some of the inconsistencies in the literature thermodynamic properties of Ni-Al alloys, including a previous study done in this laboratory by Johnston and Palmer [12] (see Section 1.1.2). The technique of Knudsen effusion mass spectrometry was used in both studies to make measurements of nickel and aluminium activities of liquid nickel-aluminium alloys.

1.1 *Previous Thermodynamic Studies*

1.1.1 *Calorimetric Measurements*

High temperature calorimetric measurements have been critically assessed by Hultgren *et al.* [13] (for solid alloys) and more recently by Desai [4] (for solid and liquid alloys). These two assessments recommend enthalpies of formation at 298 K for solid alloys, which differ by up to a maximum of 13 kJ mol^{-1} (at the NiAl composition).

1.1.2 *Activity Measurements*

Measurements of the partial molar free energy of solution of aluminium, $\Delta\overline{G}_{Al}$, and the thermodynamic aluminium activity, a_{Al}, in solid and liquid Ni-Al alloys have been made by a number of investigators. These quantities are related by the thermodynamic relationship

$$\Delta\overline{G}_{Al} = RT \ln a_{Al}$$

where R is the gas constant (8.3143 J mol^{-1} K^{-1}) and T is the temperature (K).

Steiner and Komarek [14] used an isopiestic method for determination of the aluminium activities of solid alloys with aluminium atom fraction x_{Al} between 0.20 and 0.60 over the temperature range 1200 K to 1400 K. Malkin and Pokidyshev [15] used electromotive force (emf) measurements on a high temperature galvanic cell with a molten salt electrolyte to calculate aluminium activities of solid alloys with $0.20 \le x_{Al} \le 0.25$ and $1045\ K \le T \le 1180\ K$. Both the above studies were used as the basis of the similar critical assessments by Hultgren *et al.* [13] and Desai [4] of the partial molar quantities and integral quantities for solid Ni-Al alloys at 1273 K. Gibbs energies (partial molar free energies) and activities of nickel were calculated by integration of the Gibbs-Duhem relation.

Schaeffer [16] used emf measurements on a high temperature galvanic cell with a molten salt electrolyte to calculate aluminium activities of both solid and liquid alloys with $0.70 \le x_{Al} \le 1.00$ and $957\ K \le T \le 1201\ K$. However, interaction of the electrodes with alloys containing more than 15 at.% Ni restricted reliable activity values to alloys with $x_{Al} > 0.85$, as reported by Schaeffer and Gocken [17].

Elrefaie and Smeltzer [18] used emf measurements on a high temperature galvanic cell with a solid electrolyte to calculate aluminium activities of solid nickel-rich alloys with aluminium concentration between 0.17 at.% and 2.36 at.%, in coexistence with alpha alumina at 1213 K. The value of the aluminium activity coefficient was essentially constant, corresponding to Henrian solution behaviour.

Vachet *et al.* [19] studied the partition of aluminium between liquid aluminium-nickel alloys ($0 < x_{Al} \leq 0.4$) and liquid silver to determine aluminium activities at 1873 K. Their calculations relied on determinations of the activity of aluminium in silver at much lower temperatures (973 K $\leq T \leq$ 1253 K). The critical assessment by Desai [4] for liquid Ni-Al alloys at 1873 K was based in part on these results of Vachet *et al.*, as well as the results of Schaeffer and Gocken [16, 17], and was interpolated for compositions $0.4 \leq x_{Al} \leq 0.8$. Furthermore, it should be noted that at this temperature the non-stoichiometric β-NiAl phase is still solid, rather than liquid, as the melting point is 1912 K [13] at the $x_{Al} = 0.5$ composition.

Johnston and Palmer [12] attempted to measure directly both nickel and aluminium activities for nickel-rich liquid alloys ($0.54 \leq x_{Ni} \leq 0.89$) in the temperature range 1750 K $\leq T \leq$ 2100 K, using the technique of multiple Knudsen-cell mass spectrometry. Although both nickel and aluminium ion currents were measured, only nickel activities were reported, due to materials problems associated with containment of liquid aluminium and the more aluminium-rich alloys. The nickel activities showed large negative deviations from Raoult's law, in agreement with the results of Vachet *et al.* [19] in the only other study conducted at a similar temperature on liquid alloys. However, Johnston and Palmer's nickel activities were somewhat lower than the Gibbs-Duhem calculated values of Vachet *et al.*, and Desai [4] reported that they yielded $\Delta\overline{G}_{Al}$ values which were up to 10 kJ mol^{-1} less exothermic than his recommended values.

Oforka and Argent [20, 21] determined nickel and aluminium activities for solid alloys ($0.23 \leq x_{Al} \leq 0.64$) at 1423 K by Knudsen cell mass spectrometry. They reported nickel activities significantly lower than the assessment of Hultgren *et al.* [13] at 1273 K, yet in reasonable agreement with the results of Schaeffer [16]. However, their aluminium activities for high concentrations of aluminium were in poor agreement with Schaeffer's results, and at low concentrations of aluminium their aluminium activities were significantly greater than those assessed by Hultgren *et al.* [13] or Steiner and Komarek [14].

Hilpert *et al.* [5] performed Knudsen effusion mass spectrometry measurements on solid Ni-Al alloys with $0.71 \leq x_{Ni} \leq 0.84$ and 1409 K $\leq T \leq$ 1703 K. Ni^+/Al^+ ion intensity ratios were determined and used to calculate phase boundaries in conjunction with differential thermal analysis measurements. Subsequently, Hilpert *et al.* [6] have recently published a complete thermodynamic study of the liquid and solid alloys with $0.7 \leq x_{Ni} \leq 1$ and 1389 K $\leq T \leq$ 1734 K. They determined by direct measurements chemical activities for both nickel and aluminium, and an independent method for determining the nickel activities of solid alloys yielded consistent results. They critically assessed previous studies and also determined a complete set of partial and integral thermodynamic functions for the solid phase Ni_3Al with $x_{Ni} = 0.750$ at 1600 K. This yielded the enthalpy of formation of Ni_3Al at room

temperature, $\Delta_f H_m$ (298.15 K) = - 153 ± 20 kJ mol^{-1}, in good agreement with literature calorimetric measurements.

2. *Experimental*

2.1 *Materials*

Alloys were produced by induction melting (in air) high-purity aluminium and nickel in an alumina crucible, and casting in alumina-washed steel chill moulds. The elements were chemically and spectroscopically analysed. The aluminium contained 10 ppm each of Cu, Mg and Si, and 5 ppm Fe as the major impurities, while the nickel contained 200 ppm C, 5 ppm Si, 4 ppm Cu and 1 ppm Mg. The ingots (weighing 1 to 2 kg) were sectioned with a water-cooled diamond saw and several samples (0.75 to 2 g) taken from various points along the ingot and analysed by atomic absorption spectroscopy for aluminium to verify homogeneity of the ingot composition. The ingots were the same used by Johnston and Palmer [12]. Samples of 150 to 300 mg were used for high temperature mass spectrometry and were taken from central sections of the ingots immediately adjacent to chemically analysed regions. These analyses for Ni and Al, by atomic absorption spectroscopy, are given in Table 1. The residues after each vaporization experiment were also analysed, and the analyses are given in Table 1. Composition accuracy is ± 0.005 in atom fraction x_{Ni} in all samples except S0023 and S0033, where it is ± 0.01.

2.2 *Mass Spectrometry*

The multiple Knudsen-cell mass spectrometry apparatus and techniques used were as described by Johnston and Palmer [12]. Molybdenum quad-cells were used in the present study, together with close-fitting crucible liners and lids of recrystallized alumina. An earlier study [22] had shown that graphite crucibles as used by Johnston and Palmer were unsuitable for thermodynamic studies of nickel-based alloys. Hilpert *et al.* [5] also rejected the use of glassy carbon inner cells after observing that they caused a solution of carbon in the Al/Ni alloys.

The quad-cells were modified by enlarging the former effusion holes to 1 mm diameter and countersinking them (Fig. 2). A new effusion hole of 0.5 mm diameter was ultrasonically drilled in each alumina crucible (of 1.5 mm wall thickness). Tungsten strip shims ensured alignment of the two holes. The internal diameter of the crucibles was 5 mm, giving a ratio of the evaporating surface area (taken as geometrical cross-sectional area of the cell for a liquid alloy) to effusion orifice area of 100:1.

The quad-cell was heated by electron bombardment (750 eV) from two resistively heated thoriated tungsten ribbons. These were concentric with the quad-cell (which was held at ground potential) and were independently controlled to minimize temperature gradients over the quad-cell.

Table 1: *Composition (in weight percent) and atom fraction x_{Ni} of initial and residual nickel-aluminium alloys used in Knudsen-cell mass spectrometry.*

Sample	Initial Alloy				Residual Alloy			
	Al	Ni	Total	x_{Ni}	Al	Ni	Total	x_{Ni}
S0003	27.4_8	72.3_1	99.8	0.54_7	24.3_1	75.3_9	99.7	0.58_7
S0004	17.7_0	81.8_2	99.5	0.68_0	16.6_7	83.0_8	99.8	0.69_5
S0006	13.6_3	86.0_4	99.7	0.74_4	13.5_9	85.7_1	99.3	0.73_9
S0023	13.6_3	86.0_4	99.7	0.74_4	14.1_5	84.2_4	98.4	0.72
S0009	11.4_7	88.5_3	99.9	0.78_1	11.4_0	87.8_8	99.3	0.77_5
S0033	11.4_1	88.5_3	99.9	0.78_1	14.5_1	83.6_9	98.2	0.72
S0011	8.9_0	90.8_9	99.8	0.82_4	8.8_6	91.0_7	99.9	0.82_5
S0014	5.4_0	94.6_1	100.0	0.89_0	6.2_7	92.8_9	99.2	0.86_5

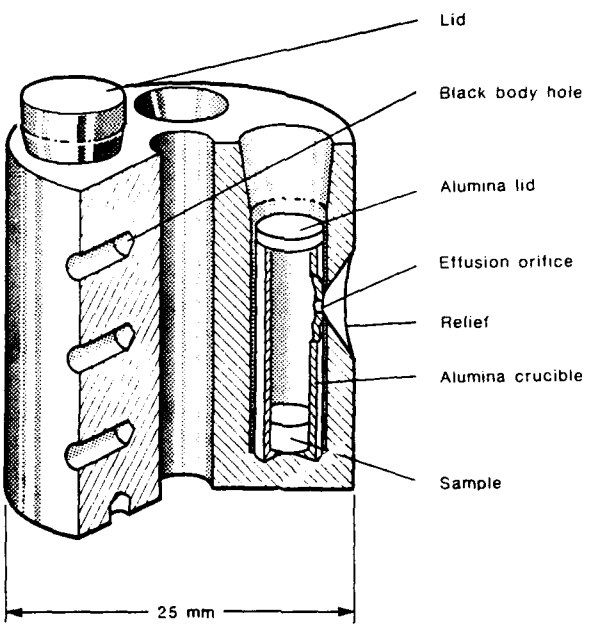

Figure 2: *Molybdenum quad-cell with alumina crucible as Knudsen cell.*

Temperatures of the blackbody holes in the quad-cell were measured with a calibrated Leeds and Northrup model 8627 disappearing filament optical pyrometer, and corrected for window transmittance. Temperature uniformity measurements were performed as described by Johnston and Burley [23] using an Ircon model 138P optical radiation pyrometer. Vertical temperature uniformity in the quad-cell was typically within ± 2 K while circumferential temperature uniformity was ± 5 K for experimental temperatures in the range 1800 K to 2100 K.

A Bendix Model MA-1 time-of-flight mass spectrometer was used to monitor the 58 Ni^+ and 27 Al^+ ion currents, using an electron energy of 35 eV and a trap current of 0.5 μA. The thermodynam, [illegible]l activity, a_{Ni}, of a nickel-aluminium alloy is given by

$$a_{Ni} = \frac{p_{Ni}}{p^{o}_{Ni}} = \frac{I_{Ni}}{I^{o}_{Ni}} \cdot \frac{S_{Ni}}{S_{alloy}} \qquad (1)$$

where p_{Ni} and p^{o}_{Ni} are the nickel vapour pressures in equilibrium with the alloy and pure nickel respectively, contained in different crucibles of the quad-cell. I_{Ni} and I^{o}_{Ni} are the ion currents for nickel vaporizing from the alloy and pure nickel respectively, and S_{Ni} and S_{alloy} are the transmission calibration factors for the respective Knudsen cells. These were determined in separate experiments using pure nickel in each cell, as described by Johnston [24].

3. *Results*

Second Law plots of ln (I^{+}_{Ni} . T) versus $1/T$ are shown in Figure 3 for a typical experiment on an alloy (S0023) and a reference sample of pure nickel, contained in adjacent Knudsen cells. Ion currents were measured at four or more temperatures in the range 1800 K to 2100 K, and the Second Law plots were analysed by the method of least squares. Calculated standard enthalpies of vaporization of pure nickel, ΔH^{o}_{298}, were generally in fair agreement (+ 5%, - 20%) with the literature value 430.1 ± 2.1 kJ mol^{-1} [25], considering the small number of data points. Ion currents were interpolated at 2000 K, and used to calculate nickel activities by equation 1.

The nickel activities at 2000 K for alloys with $0.55 \leq x_{Ni} \leq 0.89$ are shown in Figure 4 and Table 2. The reference state is liquid nickel at 2000 K. Where the initial and residual alloy compositions differ, the direction of the composition change is indicated and the curve of best fit is drawn through the average composition to which the activity is ascribed. Analyses of the initial and residual alloy compositions generally agreed to within ± 0.02 atom fraction, with the exception of sample S0033 (Table 1). Where the nickel activity was

measured twice in consecutive experiments on the same sample, the two activities are ascribed to the initial and final composition respectively. The uncertainty in the experimental activities is estimated at ± 0.05. Activities interpolated from the solid line in Figure 4, and calculated values of the activity coefficient of nickel, γ_{Ni}, where $\gamma_{Ni} = a_{Ni}/x_{Ni}$ are shown in Table 3.

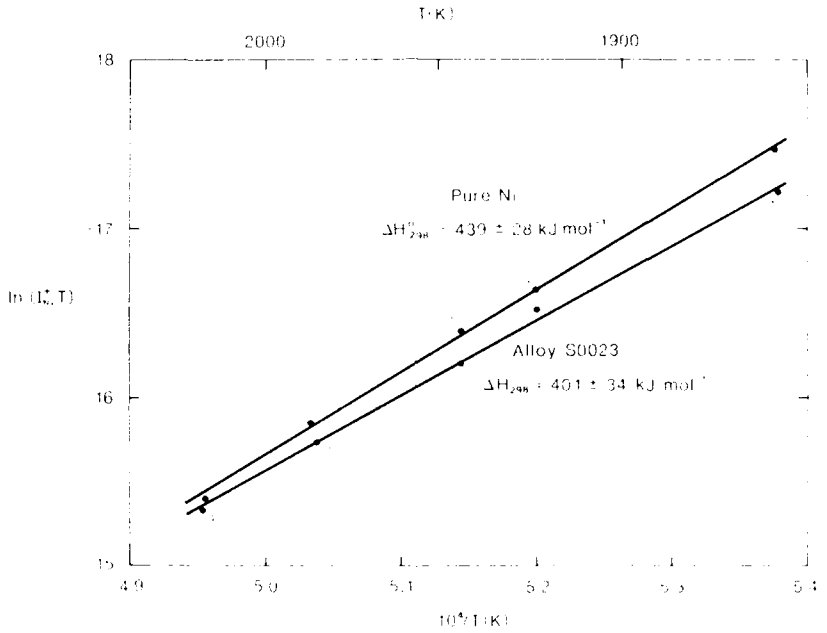

Figure 3: *Second-law plots for nickel vaporized from pure nickel and nickel-aluminium alloy (x_{Ni} = 0.74) contained in adjacent Knudsen cells. Calculated standard enthalpies of vaporization of nickel, ΔH_{298}, and 95% confidence limits are shown.*

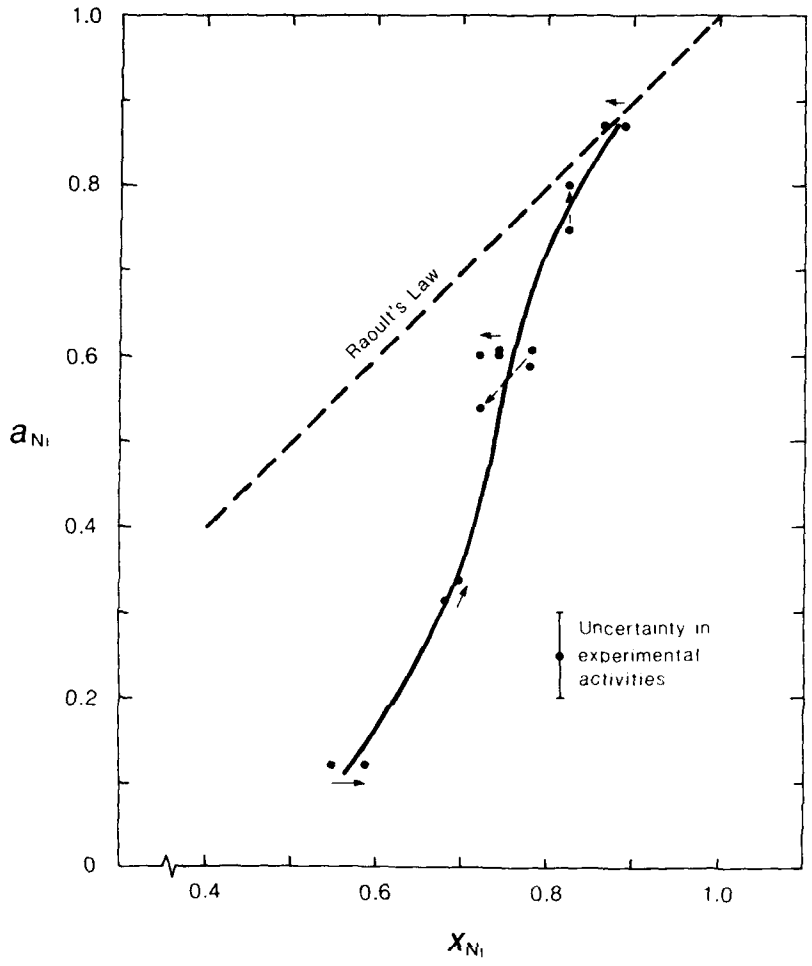

Figure 4: Nickel activity a_{Ni} as a function of atom fraction x_{Ni} in liquid nickel-aluminium alloys at 2000 K (reference state liquid nickel). Arrows show direction of composition change of alloy in single activity measurements, or change in composition and/or activity in consecutive measurements on an alloy.

Table 2: *Thermodynamic activity of nickel in liquid nickel-aluminium alloys with atom fraction x_{Ni} at 2000 K (reference state liquid nickel).*

Sample	x_{Ni}		a_{Ni}
	Initial Alloy	Residual Alloy	
S0003	0.54_7	0.58_7	0.12
S0004	0.68_0		0.31
		0.69_5	0.34
S0006	0.74_4	0.73_9	0.60
S0023	0.74_4	0.72	0.60
S0009	0.78_1	0.77_5	0.59
S0033	0.78_1		0.61
		0.72	0.54
S0011	0.82_4		0.75
		0.82_5	0.80
S0014	0.89_0	0.86_5	0.87

Table 3: *Interpolated nickel activities and activity coefficients in liquid nickel-aluminium alloys with atom fraction x_{Ni} at 2000 K (reference state liquid nickel).*

x_{Ni}	0.60	0.65	0.70	0.75	0.80	0.85	0.90
a_{Ni}	0.17	0.25	0.36	0.57	0.73	0.82	0.90
γ_{Ni}	0.28	0.38	0.51	0.76	0.91	0.97	1.00

4. Discussion

4.1 Sources of Error in Activity Measurements

4.1.1 Alignment and Temperature Errors

The large experimental scatter shown in Figure 4 reflects a number of possible sources of random error. These included movement of the crucible within the quad-cell which caused misalignment of the effusion hole and the orifice in the quad-cell, and temperature measurement errors and temperature non-

uniformity.

Relative movement of the quad-cell, the sampling holes in the tantalum heat shields and the ionizer of the mass spectrometer, due to different thermal expansions of the vacuum furnace components, was also a problem. The difficulty in reproducibly positioning the effusion hole was particularly important in view of the high degree of collimation of the molecular beam achieved with the 0.5 mm diameter by 1.5 mm long orifice. It was necessary to remove the alumina crucibles and leach them with aqua-regia to remove the residues from some experiments, and this introduced uncertainty into the calibration factor used in equation (1), through disturbance of the positioning of the effusion hole. A possible solution would have been the incorporation of a universal manipulator to allow translation of the quad-cell and thus optimization of the ion current measured for each effusion hole.

The role of temperature measurement errors in measurement of vapour pressures and enthalpies of vaporization has been discussed by Johnston and Burley [23] and Mart [22]. Appropriate measures were taken in this work to minimize both absolute temperature errors and variation of temperature between different quad-cell compartments. For thermodynamic activity measurements using multi-compartment Knudsen cells, the spatial uniformity of temperature is more important than the true temperature [12]. In the present work the ± 5 K circumferential temperature uniformity would give rise to a worst case error in calculated nickel activity of ± 0.1. In practice, the alloys and pure nickel reference were contained in adjacent cell compartments, so temperature errors and resultant nickel activity errors would be less. It is believed that temperature non-uniformity and misalignment of the crucibles were equally important contributors of error in the activity measurements, and that the calculated nickel activities are accurate to ± 0.05.

4.1.2 Effusion Orifice Condensation

The analysed initial and residual alloy compositions in Table 1 show that the alloys with the higher aluminium concentrations preferentially lost aluminium. The extent of aluminium depletion appeared to be a function of both the time at temperature and the maximum temperature attained. In several experiments it was observed that the effusion orifice in the alumina crucible became partially or fully blocked by crystals of alumina. Energy dispersive X-ray analysis of the crystals showed only the presence of aluminium; no nickel (from the NiAl sample) or molybdenum (from the quad-cell) was detected. This indicates that the crystals were not the spinel $NiAl_2O_4$. Elrefaie and Smeltzer [18] showed that the oxygen partial pressures above Ni-Al alloys in coexistence with alumina at 1273 K are many orders of magnitude lower than that of the Ni-$NiAl_{2.54}O_{4.81}$-Al_2O_3 coexistence. With increasing aluminium content of the alloy, they showed that the oxygen pressure decreased to the value corresponding to the binary Al-Al_2O_3 equilibrium. At 1273 K, for the range of compositions studied in the present work ($0.11 \leq x_{Al} \leq 0.45$), Elrefaie and Smeltzer calculated a near constant oxygen pressure of approximately 2×10^{-24} Pa, compared with 2×10^{-29} Pa for Al-Al_2O_3. Since the diffusion-pumped background pressure in the system was approximately 10^{-4} Pa in the furnace chamber, it is evident that the oxygen partial pressure was sufficiently

high for oxidation of aluminium vaporizing from Ni-Al alloys to be thermodynamically favourable. This would give rise to the gaseous aluminium oxides AlO, Al_2O, AlO_2 and Al_2O_2 which have been observed mass spectrometrically as equilibrium vapour species over condensed Al_2O_3 [26]. Formation of these vapour species in the effusion orifice, and their condensation on nucleating sites with the formation of Al_2O_3 crystals, is consistent with the observations.

The net effect of alumina growth in the effusion orifice was to decrease the measured Al^+ ion intensity, due to removal of aluminium-containing vapour species from the molecular beam. Constriction of the orifice also changed the calibration factor for both nickel vapour and aluminium vapour species.

4.1.3 *Effusion Orifice Erosion*

Another phenomenon was observed which limited the effective life of alumina crucibles. This was the erosion of the alumina surrounding the effusion orifice, where the crucible surface was exposed by the slightly larger countersunk hole in the molybdenum quad-cell. The effect was a gradual shortening of the length of the effusion orifice, and a consequent change in the calibration factor. It was not readily possible to compensate for this. Investigation revealed that the erosion process involved interaction of the alumina with molybdenum under electron bombardment, and was possibly due to electron beam induced sputtering. Heating an alumina crucible and molybdenum quad-cell combination in vacuum by induction heating for a similar time and temperature did not produce any observable volatilization of the alumina.

Scanning electron microscopy of the eroded surface from an alumina crucible exposed to electron beam heating showed a jagged surface (Fig. 5), with the peaks topped by small molybdenum-rich nodules, revealed by energy dispersive x-ray analysis (Fig. 6). Backscatter electron micrographs showed a transition region immediately around the eroded area, with a very high concentration of molybdenum-rich nodules with less-severe erosion, grading to an outer region with little erosion and lower molybdenum nodule concentration (Fig. 7). The outline of the 1 mm diameter hole in the molybdenum quad cell forms the boundary of the most eroded region on the alumina crucible.

An eroded (and alumina blocked) effusion orifice from an actual effusion experiment (NiAl sample with $x_{Al} = 0.5$) is shown in Figure 8. The outline of the 0.5 mm diameter orifice and the eroded surface of the alumina exposed by the 0.5 mm diameter hole in the misaligned quad-cell are clearly visible. The blockage of the effusion orifice was not caused by redeposition of the eroded alumina, but by oxidation of aluminium vaporizing from the sample, as discussed previously. This was indicated by other experiments when the effusion orifice blocked before substantial erosion occurred, and experiments where the converse occurred, generally with a low x_{Al} alloy.

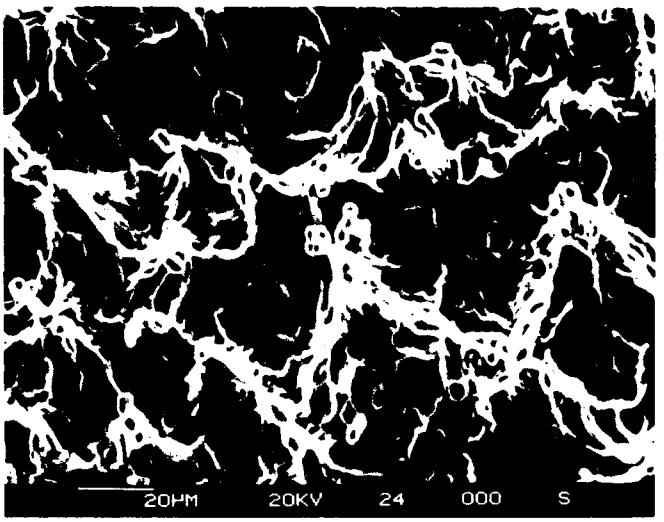

Figure 5: Scanning electron micrograph of eroded surface of alumina crucible in electron beam heated molybdenum quad-cell.

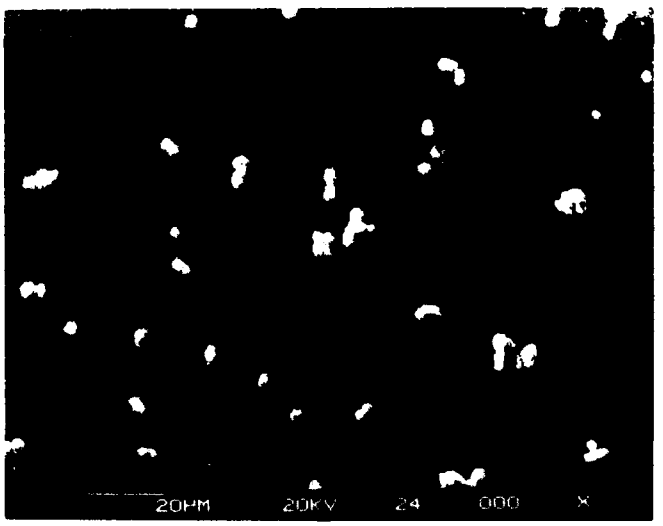

Figure 6: Energy dispersive X-ray molybdenum map of same area as Figure 4, showing molybdenum-rich nodules.

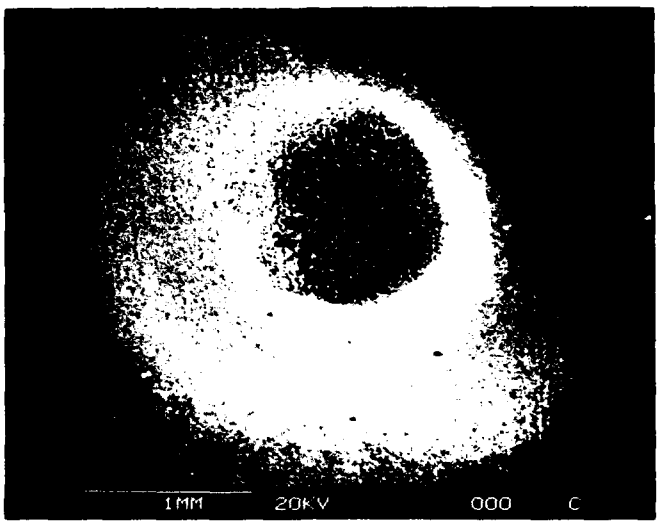

Figure 7: Backscatter electron micrograph (composition contrast) of eroded surface of alumina crucible in electron beam heated molybdenum quad-cell, showing molybdenum-rich transition region surrounding most eroded region.

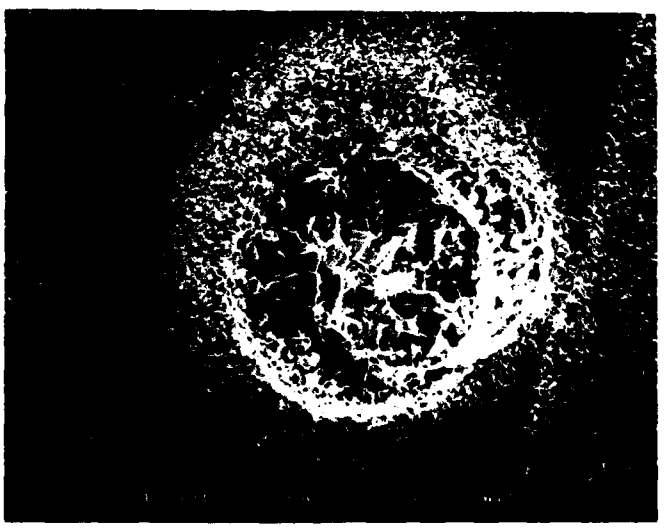

Figure 8: Scanning electron micrograph of an eroded and alumina blocked effusion orifice in an alumina crucible, contained in an electron beam heated molybdenum quad-cell.

4.1.4 *Aluminium Activity Measurements*

The problems of effusion hole blockage and erosion of the surrounding alumina imposed restrictions on the upper temperature attainable. Hole blockage was particularly prevalent for high x_{Al} samples heated for the first time; on clearing the blockage and reheating the problem usually did not recur. Frequent recalibration of the sensitivity factors compensated for the effects of gradual erosion of the effusion hole over a series of experiments. However, little reliance could be placed on Al^+ ion currents from alloys when substantial transport of aluminium oxide species was thus indicated. This was particularly so due to the use of an ionizing electron energy of 35 eV, which was sufficiently high to cause fragmentation of all Al-O vapour species. This would contribute to the observed Al^+ ion current arising from Al(g) vaporizing from the alloy, and could give rise to erroneous aluminium activities. Therefore, aluminium activities have not been calculated from Al^+ ion currents measured in the present work.

After the present experimental work was completed the work of Hilpert *et al.* [5, 6] was published. These authors rejected the use of inner cells of alumina after observing that alumina generates Al^+ ion intensities at the temperature of the Al-Ni measurements, which reduced the sensitivity of the instrument for the detection of Al partial pressures. They overcame the problem of interfering Al^+ background ion intensities by using high density calcia-stabilized zirconia inner cells.

4.2 *Comparison of Nickel Activities with Literature Values*

The nickel activities calculated in the present study are compared in Figure 9 with literature values for liquid alloys. The present results are in fair agreement with the activities reported by Vachet *et al.* [19], who determined aluminium activities for liquid alloys at 1873 K, and calculated nickel activities by the Gibbs-Duhem equation. The assessment by Desai [4] gives nickel activities identical to those of Vachet *et al.* over this composition range.

Also shown in Figure 9 are the recent Knudsen effusion mass spectrometry results of Hilpert *et al.* [6] who measured both nickel and aluminium activities at 1728 K. Their nickel activities are somewhat higher than those of Vachet *et al.* Hilpert *et al.* performed pressure calibration by vaporizing pure nickel before and after each alloy sample, and the mean value of the enthalpy of vaporization of nickel obtained from nine independent runs was in good agreement with the literature value. This (Second Law agreement) was asserted to demonstrate the accuracy of their measurements. However, there are inconsistencies between their quoted pressure calibration factors, ion intensities and calculated partial pressures. Nickel activities recalculated from their partial pressure data are higher than reported and for $x_{Ni} \geq 0.85$ exceed that expected for ideal Raoultian behaviour. It is concluded that there are errors in their pressure calibration (which do not affect Second Law agreement) resulting in high nickel activities in comparison to the results of Vachet *et al.*

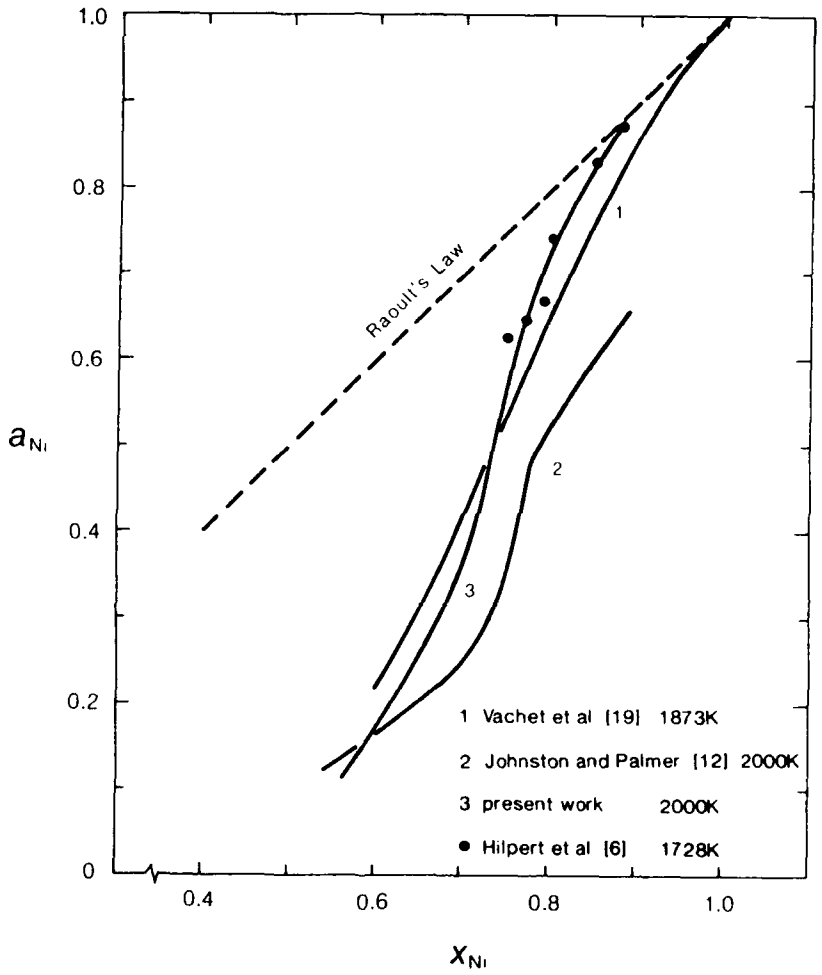

Figure 9: *Comparison of nickel activities a_{Ni} from present work with literature values for liquid nickel-aluminium alloys (reference state liquid nickel).*

4.2.1 *Effect of Graphite Container Interactions*

The present values of a_{Ni} show a smaller negative deviation from Raoult's law behaviour than do the activities previously reported by Johnston and Palmer [12], for alloys of the same composition also at 2000 K. These authors used graphite quad-cells which have been shown [22, 5] to be unsuitable for thermodynamic studies of nickel-based alloys, due to carbon solubility reducing the nickel enthalpy of vaporization and the nickel activity. Phase equilibria in the ternary nickel-aluminium-carbon system at 1273°C have been determined by Schuster and Nowotny [27]. They showed that Ni_3AlC_x does not exist as a distinct ternary phase, but that γ-Ni_3Al exhibits a solubility for carbon of up to 7 to 8 at.%. The phase β-NiAl was also found to dissolve carbon to about 3 at.%, but no solubility was detected in the phases Ni_2Al_3 and $NiAl_3$.

Re-examination of the chemical analyses of sample residues from the experiments of Johnston and Palmer [28] shows probable substantial contamination by carbon. The sum of the analysed nickel and aluminium weight percents differ from 100% by up to 4 wt.%, with the difference increasing with nickel content to a maximum at pure nickel.

If this difference is attributed to carbon dissolved in the solid phases, or precipitated from the melt, an overall carbon concentration of 17 at.% is calculated for pure nickel cooled from 1953 K, the maximum temperature of Johnston and Palmer's mass spectrometry experiment. This compares with the maximum solubility of carbon in nickel of 25 at.%, which is the composition of the metastable phase Ni_3C [29]. The chemical analyses of nickel-aluminium sample residues from the same experiment would indicate the following carbon concentrations for the respective nominal nickel atom fractions: x_{Ni} 0.89, 16 at.%C, x_{Ni} 0.74, 10 at.%C, x_{Ni} 0.55, 6 at.%C. The latter two concentrations are approximately 3 at.% higher than the concentrations determined by Schuster and Nowotny [27] at the considerably lower temperature of 1273 K.

4.2.2 *Excess Stability Function and "Cluster" Formation*

The large scatter in the experimental nickel activity values in the present work prevented calculation of the excess stability function [30], for which Johnston and Palmer [12] found a pronounced peak at $x_{Ni} = 0.75$ for liquid alloys at 2000 K. They proposed that this was evidence of the strong tendency for the formation of Ni_3Al 'clusters' in the liquid phase, at a temperature approximately 300 K higher than the melting point for this composition [13].

In view of the circumstantial evidence for carbon contamination of their samples, it seems more likely that the peak in the excess stability function actually reflects the enhanced stability of Ni_3AlC_x. Whereas Schuster and Nowotny [27] found no distinct ternary phase at 973 K or 1273 K, Han and Choo [31] in a study of rapidly solidified Ni_3Al-C alloys found that the ordered fcc single phase Ni_3AlC_x ($0 < x < 0.34$) was formed. Thus, the maximum solubility of carbon in γ-Ni_3Al was about 7.8 at.%. They found that enhanced ordering of the γ-Ni_3Al occurred, and considered that this was due to cooperative ordering of substitutional atoms (nickel and aluminium) and interstitial carbon atoms to form the $L'1_2$ type Ni_3AlC_x perovskite structure. Briant and Huang [32] in a study of rapidly solidified Ni_3Al found that carbon

segregated to the grain boundaries to an extent proportional to the bulk carbon concentration, reaching a maximum of 8.2 at.% for an alloy of nominal composition $(Ni_{76}Al_{24})_{98.5}C_{1.5}$.

The indirect evidence is that Johnston and Palmer's data [12] pertain to liquid Ni-Al alloys containing dissolved carbon. The peak in the excess stability function at $x_{Ni} = 0.75$ would then indicate that there is a strong tendency for the formation of Ni_3Al 'clusters', stabilized by dissolved carbon to a concentration of up to about 10 at.% (i.e. composition Ni_3AlC_x with $x = 0.44$).

Unfortunately the present results are unable to confirm whether or not Ni_3Al 'clusters' occur in the absence of carbon. However, calculations made using the data of Vachet *et al.* [19] show that the excess stability at 1873 K varies in a nearly linear manner from 230 kJ at $x_{Ni} = 0.6$ to 150 kJ at $x_{Ni} = 1.0$. The positive sign and magnitude of the excess stability are in fair agreement with the values observed by Johnston and Palmer [12] at each end of their similar composition range. However, there is no evidence of a peak at $x_{Ni} = 0.75$ in the excess stability function for Vachet's carbon-free alloys, which were equilibrated in alumina crucibles. It therefore appears that carbon is necessary to stabilize Ni_3Al 'clusters' in the liquid alloys.

Levin and Ayushina [33] measured the viscosity, molar volume, and surface energy of liquid Ni-Al alloys ($0 < x_{Al} < 1$) at 1923 K including those with the compositions of the compounds Ni_3Al, NiAl, Ni_2Al_3 and $NiAl_3$. They found evidence of strong interaction between nickel and aluminium atoms, with the viscosity rising to a sharp maximum at the equiatomic NiAl composition. The viscosity at the Ni_3Al composition was one quarter that of the NiAl composition, while the viscosity at the Ni_2Al_3 and $NiAl_3$ compositions were 0.6 and 0.3 respectively that of the NiAl composition. The surface energy decreased in a non-uniform manner from nickel to aluminium, with a pronounced inflection between 50 and 75 at.% Al. The molar volume over the whole range of compositions showed negative deviations from ideal behaviour, with contractions at the Ni_3Al, NiAl, Ni_2Al_3 and $NiAl_3$ compositions of approximately 11%, 16%, 18% and 15% respectively.

Levin and Ayushina concluded that the behaviour of the structurally-sensitive properties of liquid Ni-Al alloys was associated with the formation of 'micro-groupings', the composition of which is near equiatomic. Closer examination of their results shows that there may also be some tendency for the formation of micro-groupings at the Ni_2Al_3 and $NiAl_3$ compositions, but with significantly less interaction than at the NiAl composition. However, the Ni_3Al composition shows the least tendency for micro-grouping formation. These results therefore substantiate the lack of evidence from the thermodynamic results of Vachet *et al.* [19] for the existence of Ni_3Al 'clusters' in the liquid alloys.

The apparent need for dissolved carbon to stabilize Ni_3Al 'clusters' in molten Ni-Al alloys has a practical significance. As mentioned in the Introduction, γ'-Ni_3Al phase precipitation in nickel-base superalloys is crucial to their high-temperature strength and creep resistance. Although the strength of pure γ'-Ni_3Al increases with temperature, it is extremely brittle, which limits exploitation of its high-temperature strength.

Aoki and Izuma [34] reported that adding a small amount of the interstitial element boron to Ni_3Al greatly reduced the extent of intergranular fracture. As discussed by Briant and Huang [32], it is now generally accepted that boron improves ductility by segregating to the grain boundaries and improving the

cohesive strength, but the exact mechanism is still unclear. Huang *et al.* [35] reported that by rapid solidification up to 1.5 at.% boron can be held in solution in the aluminide, before formation of the $M_{23}B_6$ boride. They also showed that boron is a particularly potent strengthener in Ni_3Al, due to the large lattice strain that it produces by occupying the interstitial lattice positions, in comparison with substitutional elements such as Fe, Cr, Ti and Si.

Huang *et al.* [36] showed that carbon additions had a similar strengthening effect on Ni_3Al, typical of interstitial elements, but little effect on ductility. Briant and Huang [32] noted that the segregation of the interstitial elements boron and carbon appeared to be different, as carbon segregated to the grain boundaries to an extent only proportional to the bulk carbon concentration, whereas Liu *et al.* [37] had reported that the amount of boron on the grain boundaries was greater in nickel-rich alloys.

It would appear likely that the rapid solidification of the carbon-stabilized Ni_3Al 'clusters' in molten Ni-Al alloys forms the ordered $L'1_2$ Ni_3AlC_x perovskite structure observed by Han and Choo [31], with a maximum solubility of carbon of about 8 at.%. Briant and Huang [32] used melt spinning in vacuum with a ribbon cooling rate of $< 5 \times 10^5$ K/s. Han and Choo used a hammer-and-anvil rapid solidification apparatus with a cooling rate estimated at $< 10^4$ K/s. It is apparent that the maximum carbon segregation to the grain boundaries observed by Briant and Huang corresponds to the maximum carbon solubility in Ni_3Al observed by Han and Choo, in the single phase Ni_3AlC_x perovskite. It is interesting to postulate that the different segregation behaviour of B and C may be due to the absence of an analogous Ni_3AlB_x solidification mechanism, perhaps due to the absence of boron-stabilized Ni_3Al 'clusters' in molten Ni-Al alloys.

4.2.3 *Standard States and Nickel Activities of Solid Alloys*

It is not valid to quantitatively compare the nickel activities measured in the present work for liquid alloys at 2000 K with literature activities for solid alloys at much lower temperatures. However, qualitative comparisons can be made and inconsistencies in the literature data resolved.

Different standard states have been used by different authors, leading to confusion in reporting and comparison of nickel activities for solid nickel-aluminium alloys. Oforka and Argent [20, 21] reported that their nickel activities at 1423 K (with standard state solid nickel) were in reasonable agreement with the results of Schaeffer [16], but significantly lower than those assessed by Hultgren *et al.* [13] at 1273 K. However, Schaeffer did not obtain experimental results in this composition range ($0.396 < x_{Ni} < 1.0$), but reported the data of Hultgren *et al.* (standard state solid nickel) adjusted to the standard state of liquid nickel. Therefore the apparent agreement between Oforka and Argent's results and those of Schaeffer is erroneous.

A further discrepancy exists in Oforka and Argent's aluminium activities at low x_{Al} which are significantly greater than the values obtained by Steiner and Komarek [14] or assessed by Hultgren *et al.* [13]. Oforka and Argent used alumina Knudsen cells with which they experienced 'degassing' problems. They used an ionizing electron energy of 35 eV which, as has been shown in the present work, is sufficient to cause fragmentation of Al-O vapour species

emanating from the Knudsen cell. As discussed by Hilpert *et al.* [5], this would give rise to anomalously high Al^+ ion currents particularly for alloys of high nickel content, and could explain the high aluminium activities observed.

Oforka and Argent reported that these nickel and aluminium activities were consistent by integration, but recalculation using their data shows that this is incorrect. There are significant differences between the nickel activities obtained by integration of their aluminium activity data, and the nickel activities that they measured by experiment. For the above reasons, the nickel activities of solid Ni-Al alloys reported by Oforka and Argent are considered less reliable than those in the assessment of Hultgren *et al.* [13]. As previously mentioned in Section 1.1.2, there are only slight differences in the nickel activities for solid Ni-Al alloys at 1273 K, assessed by Hultgren *et al.* and more recently by Desai [4]. To emphasize the discrepancy between the results of Oforka and Argent, and these two assessments, one may compare the activities in corresponding two phase regions. For a binary system, the Phase Rule dictates that the activities are constant in a two phase region at a particular fixed temperature. Thus for the two phase Ni_3Al and NiAl coexistence, the nickel and aluminium activities measured by Oforka and Argent are respectively 0.53 and 5.12 times those assessed by Desai.

5. *Conclusions*

In this report nickel activities for binary liquid Ni-Al alloys have been measured at 2000 K in alumina Knudsen cells. While the experimental reproducibility was poor, it was confirmed that in the concentration range studied, $0.55 \leq x_{Ni} \leq 0.89$, the activity of nickel shows large negative deviations from Raoult's Law, in agreement with the study by Vachet *et al.* [19] at 1873 K. The results are also qualitatively consistent with the literature activities for solid Ni-Al alloys, which show similar negative deviations from Raoult's Law. This indicates the strong attraction between the unlike nickel and aluminium atoms, in both solid and liquid Ni-Al alloys.

While the present results did not permit calculation of the excess stability function, and evidence for or against 'cluster' formation at $x_{Ni} = 0.75$ in the binary alloys, circumstantial evidence points to the presence of carbon being necessary to stabilize Ni_3Al 'clusters' in the liquid alloys.

6. *Acknowledgements*

The authors wish to acknowledge the contributions to this study of Mr F.A. Griffo, who machined the alumina Knudsen cells, Mr I.G. McDonald, who performed the chemical analyses, and Mrs V.M. Silva, who performed the SEM analyses.

7. *References*

1. Hansen, M. and Anderko, K. (1958).
   Constitution of binary alloys, pp. 118-121. New York: McGraw-Hill.

2. Elliott, R.P. (1965).
   Constitution of binary alloys, First Supplement, p. 48. New York: McGraw-Hill.

3. Shunk, F.A. (1969).
   Constitution of binary alloys, Second Supplement, p. 31. New York: McGraw-Hill.

4. Desai, P.D. (1987).
   Thermodynamic properties of selected binary aluminium alloy systems. *Journal of Physics and Chemistry Reference Data*, **16** (1), 109-124.

5. Hilpert, K., Kobertz, D., Venugopal, V., Miller, M., Gerads, H., Bremer, F.J. and Nickel, H. (1987).
   Phase diagram studies on the Al-Ni system. *Z. Naturforsch.* **42a**, 1327-1332.

6. Hilpert, K., Miller, M., Gerads, H. and Nickel, H. (1990).
   Thermodynamic study of the liquid and solid alloys of the nickel-rich part of the Al-Ni phase diagram including the $AlNi_3$ phase. *Ber. Bunsenges, Phys. Chem.*, **94**, 40-47.

7. Bremer, F.J., Beyss, M., Karthaus, E., Hellwig, A., Schober, T., Welter, J.-M. and Wenzl, H. (1988).
   Experimental analysis of the Ni-Al phase diagram. *Journal of Crystal Growth*, **87**, 185-192.

8. Schramm, J. (1941).
   Z. Metallkunde, **33**, 347-355.

9. Meetham, G.W. (1982).
   Superalloys in gas turbine engines. *Metallurgist and Materials Technology*, 387-391.

10. Pettit, F.S. (1983).
    Gas turbine applications. In, E. Lang (ed.) *Coatings for high temperature applications*, pp. 341-360. London: Applied Science Publishers.

11. Helms, H.H. and Rozner, A.G. (1970).
    Pyrotechnic compositions containing nickel and aluminium. US Patent 3, 503, 814.

12. Johnston, G.R. and Palmer, L.D. (1980).
Quad-cell mass spectrometry: thermodynamic properties of liquid aluminium-nickel alloys. *High Temperature - High Pressure*, **12**, 261-266.

13. Hultgren, R., Desai, P.D., Hawkins, D.T., Gleiser, M. and Kelly, K.K. (1973).
Selected values of the thermodynamic properties of binary alloys, pp. 191-195.
ASM, Metals Park, Ohio.

14. Steiner, A. and Komarek, K.L. (1964).
Thermodynamic activities of solid nickel-aluminium alloys. *Transactions of the Metall. Soc. AIME*, **230**, 786-790.

15. Malkin, V.I. and Pokidyshev, V.V. (1965).
Study of the nature of the interaction between the components in the γ- and γ'-phase of the systems Ni-Al, Ni-Al-Cr, Ni-Al-Co, and Ni-Al-Fe. *Izv. Akad. Nauk SSSR Neorg. Mater.*, **1**, 1747-1757.

16. Schaefer, S.C. (1975).
Thermodynamic properties of the Al-Ni system. Report of Investigations 7993.
Washington: US Bureau of Mines.

17. Schaefer, S.G. and Gocken, N.A. (1979).
Thermodynamic properties of liquid Al-Ni and Al-Si systems. *High Temperature Science*, **11**, 31-39.

18. Elrefaie, F.A. and Smeltzer, W.W. (1981).
Thermodynamics of nickel-aluminium-oxygen system between 900 and 1400 K. *Journal of the Electrochemical Society*, **128** (10), 2237-2242.

19. Vachet, F., Desre, P. and Bonnier, E. (1965).
Determination of the activity of aluminium in the liquid alloys (Al, Fe); (Al, Co); (Al, Ni) at 1600°C. *C.R. Acad. Sci.*, **260**, 453-456.

20. Oforka, N.C. and Argent, B.B. (1985).
Thermodynamics of Ni-Cr-Al alloys. *Journal of Less-Common Metals*, **114**, 109.

21. Oforka, N.C. (1986).
Thermodynamics of aluminium-nickel alloys. *Indian Journal of Chemistry*, **25A**, 1027-1029.

22. Mart, P.L. (1983).
Influence of container interactions on the vaporization thermodynamics of nickel (Report MRL-R-884). Maribyrnong, Vic.: Materials Research Laboratory.

23. Johnston, G.R. and Burley, N.A. (1977).
Quad-cell mass spectrometry: vaporization studies up to 2300 K using a rotatable, multiple Knudsen cell ('quad-cell'). In, A. Cezairliyan (ed.)
Proceedings of the Seventh Symposium on Thermophysical Properties,
pp. 222-230. New York: American Society of Mechanical Engineers.

24. Johnston, G.R. (1977).
High temperature vaporization studies using quad-cell mass spectrometry. In, D. Price and J.E. Williams (eds.) *Dynamic Mass Spectrometry*, Volume 5, pp. 206-215. London: Heydon.

25. Hultgren, R., Desai, P.D., Hawkins, D.T., Gleiser, M., Kelley, K.K. and Wagman, D.D. (1973).
Selected values of the thermodynamic properties of the elements, pp. 350-357. ASM, Metals Park, Ohio.

26. Farber, M., Srivastava, R.D. and Uy, O.M. (1972).
Mass spectrometric determination of the thermodynamic properties of the vapour species from alumina. *Journal of the Chemical Society, Faraday Transactions, I.* **2**, 249-258.

27. Schuster, J.C. and Nowotny, H. (1982).
The ternary system nickel-aluminium-carbon. *Monatschefte fur Chemie*, **113**(2), 163-170.

28. Johnston, G.R. and Palmer, L.D. (1980).
Unpublished results. MRL High Temperature Properties Group.

29. Ponyatovskii, E.G., Aptekar, I.L. and Ershova, T.P. (1966).
The phase diagram of the system nickel-carbon. *Dokl. Akad. Nauk SSSR*, **171**(4), 919-922.

30. Darken, L.S. (1967).
Thermodynamics of binary metallic solutions. *Transactions of the Metall. Society AIME*, **239**, 80-89.

31. Han, K.H. and Choo, W.K. (1983).
Carbon effect on ordering of γ-Ni_3Al in rapidly solidified Ni_3Al-C alloys. *Scri. Metall.*, **17**, 281-284.

32. Briant, C.L. and Huang, S.C. (1986).
Carbon segregation to grain boundaries in rapidly solidified Ni_3Al. *Met. Transactions A*, **17A**, 2084-2086.

33. Levin, E.S. and Ayushina, G.D. (1971).
Some physico-chemical properties of nickel-aluminium melts. *Izv. Akad. Nauk SSSR, Metally.* (1), 227-229.

34. Aoki, K. and Izumi, O. (1979).
Improvement in room temperature ductility of the Ll_2 type intermetallic compound Ni_3Al by boron addition. *Journal of Japanese Institute of Metals*, **43**, 1190-1196.

35. Huang, S.C., Taub, A.I. and Chang, K.M. (1984).
Boron extended solubility and strengthening potency in rapidly solidified Ni_3Al. *Acta Metall.*, **32**(10), 1703-1707.

36. Huang, S.C., Briant, C.L., Chang, K.M., Taub, A.I. and Hall, E.L. (1986). Carbon effects in rapidly solidified Ni_3Al. *Journal of Mater. Research*, **1**, 60-67.

37. Liu, C.T., White, C.L. and Horton, J.A. (1985). Effect of boron on grain-boundaries in nickel-aluminium (Ni_3Al). *Acta Metall.*, 33(2), 213-229.

SECURITY CLASSIFICATION OF THIS PAGE **UNCLASSIFIED**

DOCUMENT CONTROL DATA SHEET

REPORT NO.	AR NO.	REPORT SECURITY CLASSIFICATION
MRL-TR-91-15	AR-006-366	Unclassified

TITLE

High temperature mass spectrometric study of the thermodynamics of liquid nickel-aluminium alloys at 2000 K

AUTHOR(S)
Peter L. Mart and Warren D. Reid

CORPORATE AUTHOR
Materials Research Laboratory
PO Box 50
Ascot Vale Victoria 3032

REPORT DATE	TASK NO.	SPONSOR
May, 1991	DST 86/092	DSTO

FILE NO.	REFERENCES	PAGES
G6/4/8-3607	37	31

CLASSIFICATION/LIMITATION REVIEW DATE

CLASSIFICATION/RELEASE AUTHORITY
Chief, Materials Division

SECONDARY DISTRIBUTION

Approved for public release

ANNOUNCEMENT

Announcement of this report is unlimited

KEYWORDS

(Alloy) Thermodynamics	Mass Spectrometry	Knudsen
Nickel	Aluminium	Activity

ABSTRACT

This report describes a study of the thermodynamic properties of liquid nickel-aluminium alloys, using the technique of Knudsen effusion mass spectrometry. In the concentration range studied, $0.55 \leq x_{Ni} \leq 0.89$, the activity of nickel at 2000 K shows large negative deviations from Raoult's law, which is indicative of the strong attraction between the nickel and aluminium atoms.

The role of container interactions in affecting thermodynamic parameters derived from Knudsen cell measurements is highlighted, and inconsistencies in earlier investigations are discussed.